Jurnal Teknologi

Full Paper

MODELLING OF CAPACITIVE POWER TRANSFER SYSTEM BASED ON CLASS-E LCCL TOPOLOGY

Cheok Yan Qi, Yusmarnita Yusop*, Shakir Saat, Huzaimah Husina, Izadora

Advance Sensors & Embedded Control System (ASECS) Research Group, Faculty of Electronics & Computer Engineering, Universiti Teknikal Malaysia Melaka, Melaka, Malaysia

Article history
Received
22 October 2021
Received in revised form
23 January 2022
Accepted
26 January 2022
Published Online
20 April 2022

*Corresponding author
yusmarnita@utem.edu.my

Graphical abstract

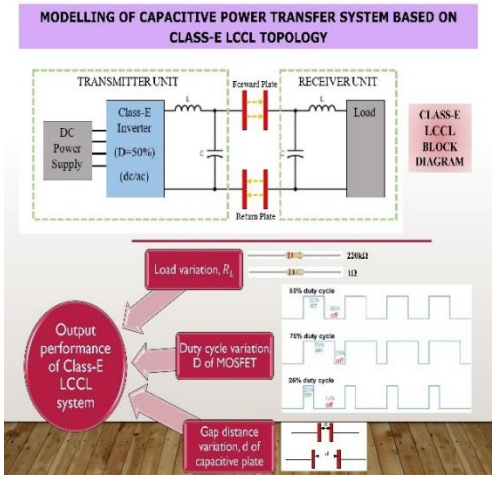

Abstract

Nowadays, capacitive power transfer (CPT) is becoming increasingly popular technology in the wireless charging field due to its better mobility and higher durability. This paper proposed a CPT system by using Class-E inverter. This topology is selected due to its ability to achieve 100% efficiency theoretically. L-match impedance matching circuits are applied at both transmitter and receiver part to allow the load impedance to match with the source impedance to maximize the power transfer. The proposed CPT system is designed and simulated by using Simulink in MATLAB software. Its output performances are analyzed. Besides, the designed CPT system is used to investigate the factors that affect its output performance by varying the load, duty cycle and gap distance between coupling plates. From this work, the proposed CPT system produced up to 97.35% efficiency and output power of 10W.

Keywords: Capacitive power transfer, Class-E inverter, Duty cycle variation, Gap distance variation, Impedance matching, Load variation, Zero-voltage switching (ZVS)

Abstrak

Pada masa kini, pemindahan kuasa kapasitif (CPT) menjadi teknologi yang semakin popular dalam bidang pengecasan tanpa wayar kerana mobilitinya yang lebih baik dan ketahanan yang lebih tinggi. Kertas ini mencadangkan sistem CPT dengan menggunakan penyongsang Kelas-E. Topologi ini dipilih kerana keupayaannya untuk mencapai kecekapan 100% secara teori, litar padanan impedans L digunakan pada bahagian pemancar dan penerima untuk membolehkan galangan beban dipadankan dengan galangan sumber untuk memaksimumkan pemindahan kuasa. Sistem CPT yang dicadangkan direka bentuk dan disimulasikan dengan menggunakan Simulink dalam perisian MATLAB. Prestasi keluarannya dianalisis. Selain itu, sistem CPT yang direka bentuk digunakan untuk menyiasat faktor-faktor yang mempengaruhi prestasi keluarannya dengan mempelbagaikan beban, kitaran tugas dan jarak jurang antara plat gandingan. Daripada kerja ini, sistem CPT yang dicadangkan boleh menghasilkan kecekapan tinggi sehingga 97.35% dan kuasa output 10W.

Kata kunci: Pemindahan daya kapasitif, Penyongsang Kelas-E, Variasi kitaran tugas, Variasi jarak jurang, Pemadanan Impedansi, Variasi beban, Pertukaran voltan sifar (ZVS)

1.0 INTRODUCTION

In this new era of technology, the wireless power transfer (WPT)[1], [2] technology is being greatly explored since there is high demand from public. WPT enables power to transfer from the source to load without physical connectors or wires. Consequently, WPT system reduces the use wires and batteries.

The WPT consists of three parts, namely transmitter unit, energy medium transfer and receiver unit. The resonant power converter[3] in the transmitter unit is connected to a power source. It converts DC power to high frequency AC power which is then transferred across the energy medium transfer to the receiver unit. The rectifier at the receiver unit rectifies[4] the received AC power to DC power so it can be used by load. The energy medium transfer is the distance between the transmitter and the receiver. It can be air or dielectric material. Figure 1 shows the general block diagram of the WPT system.

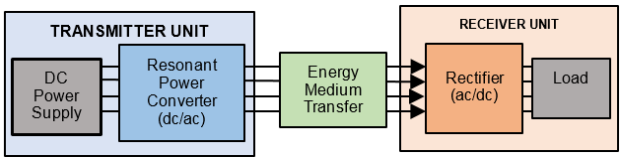

Figure 1 Block Diagram of WPT System

The WPT can be roughly divided into two regions which is near-field(non-radioactive region) [5], [6] and far-field(radioactive region)[7], [8]. Currently, near-field technology of WPT is more reliable and safer in transferring power as it does not contain radioactive elements. Two categories which are more popular in the near-field technology of WPT are Capacitive Power Transfer (CPT) [9] and Inductive Power Transfer (IPT)[10]. In near field, the power transferred over a short distance by electric field using capacitive coupling between the metal electrodes in CPT or by magnetic field between the inductive coils in IPT. However, IPT is sensitive to metal barrier. When there is metal exists in between the power source and load in IPT system, a magnetic field will generate in the system which causes power loss. CPT technique is proposed to overcome this limitation of the IPT system due to its nature of using electric fields which is not sensitive to the presence of any metals. Besides, the IPT system utilizes high-cost Litz wire coils to transfer power, while the CPT system utilizes metal electrodes to transfer power which is cheaper. In addition, the topology of CPT is simpler than IPT system.

Figure 2 shows the block diagram of CPT system. The operation of CPT system is similar to the WPT system. However, CPT system utilizes metal plates such as copper and platinum as capacitive coupling plates and placed between the transmitter and receiver side. When current passes through the metal plates, electric field is induced. The electric field carries the energy from the first metal plate at the transmitter unit to another metal plate of the receiver unit.

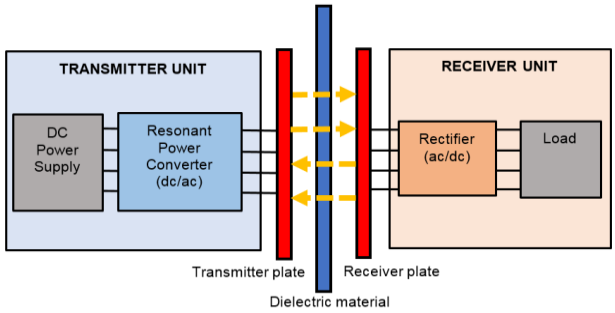

Figure 2 Block Diagram of CPT System

A dielectric material[11] is inserted between the metal plates in order to avoid them from close contact with each other. The dielectric material is an insulator or a poor conductor that can be polarized when applied with an electric field. Dielectric materials can be air, vacuum, liquid, gas, porcelain (ceramic), mica, plastics, glass, and oxides of materials. By adding a dielectric material, it increases the capacitance of both metal plates which resulting in increasing the storage of charges on metal plates.

CPT is widely used for charging application in various fields. For example, the CPT system is used for charging electronic implanted device [12], [13] in biomedical field, electric vehicles [14], [15], [16], [17] , aircraft [18] and drones [19]. CPT system can also be designed for rotary application [20] such as wireless charging for multi-rotor.

In this paper, the proposed CPT system utilizes the topology of Class-E amplifier. It is also known as Class-E inverter due to the existence of LC resonant circuit connected in series at the output of the amplifier. Class-E inverter is selected because it can achieve zero-voltage switching (ZVS) and yield 100% efficiency theoretically. Besides, the Class-E inverter is simpler and cheaper to construct compared to other classes of resonant inverter because it consists of only one active switch, S as shown in Figure 3.

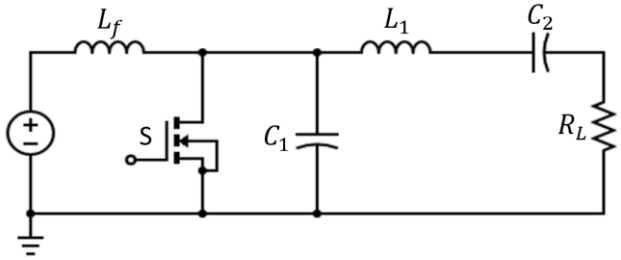

Figure 3 Class-E inverter

Class-E inverter consists of a choke inductor L_f, a metal-oxide semiconductor field-effect transistor (MOSFET), a shunt capacitor C_1, and a $L_1{-}C_2{-}R_L$ series resonant circuit. The choke inductor reduces the ripple current and provide DC current flow to the circuit. In this case, the MOSFET acts as a switch while the shunt

capacitor removes unwanted harmonics in the circuit. The $L_1-C_2-R_L$ series resonant circuit converts the digital input signal into sinusoidal output with zero DC offset.

The Class-E inverter belongs to a family of soft switching inverters. During soft switching, the switch voltage, V_{ds} falls to zero before the MOSFET turns on and off. When the MOSFET turns on, the switch current, I_d flows through the MOSFET. Since the switch current and voltage waveform does not overlap with each other during the switching time intervals as shown in the Figure 4, there is no switching loss, which means the ZVS condition is achieved. Thus, the Class-E inverter can yield 100% efficiency theoretically.

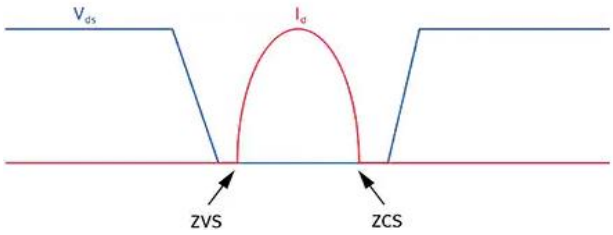

Figure 4 Waveform of switch current and voltage at ZVS condition

The following statement states the scope of this paper:

I. The CPT system is limited to the applications of low wattage charging and small gap distance only. For the proposed CPT system, output power P_{out} of 10W is obtained and it is sufficient for the application in LED driving, charging mobile devices such as mobile phones and tablets and USB interface.

The following statements describe the problem statements of this paper:

I. For low wattage applications, CPT systems exhibited limited output power and efficiency especially when the gap distance increases.

II. The output performance of the CPT system such as efficiency is affected by duty cycle, load, and gap distance between coupling plates. CPT techniques are generally applicable in very small to small gap regions (<2mm).

The following statements describe the main contributions of this paper:

I. The proposed CPT system was designed and simulated using MATLAB. It consists of resonant Class-E inverter with LCCL impedance matching network that allows maximum power transfer from source to load. The Class-E inverter is powered by DC power supply at 24V, operates at 1MHz frequency to generate the required output power of 5V with the load resistance, R_L equal to 50Ω.

II. Three factors, namely load variation, duty cycle variation and gap distance variation between coupling plates that can affect the output performance of the proposed CPT system were examined to determine the specification that will allow maximum power transfer from source to loads.

This paper is divided into four sections. Section 2 presents the design and simulation of the Class E inverter with LCCL impedance matching circuit using MATLAB. Section 3 describes the output performance of the proposed CPT system at selected resonant frequencies. The effects of varying load, duty cycle, and gap distance between coupling plates are also shown in this section. The last section, which is section 4, summaries the findings in this paper.

2.0 METHODOLOGY

The proposed CPT system is designed by using Simulink in MATLAB software. Figure 5 shows the block diagram of the proposed CPT system while Figure 6 shows the flow chart of designing the CPT system.

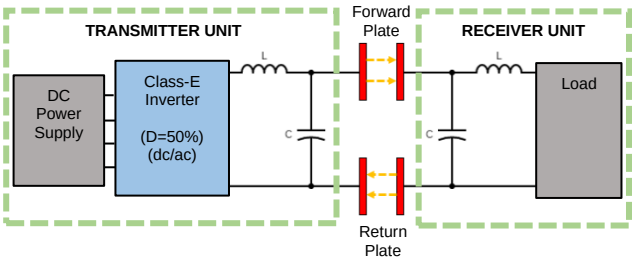

Figure 5 Block Diagram of Proposed CPT System

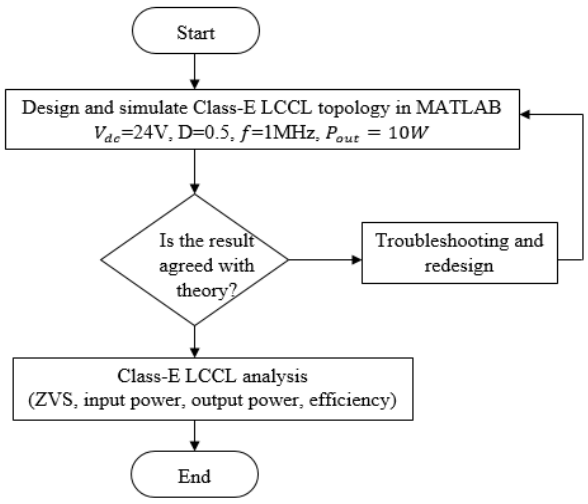

Figure 6 Flow Chart of Proposed CPT System

By referring to Figure 5, the system consists of a transmitter unit, capacitive coupling plates, and a receiver unit. Class-E inverter is applied on the transmitter unit to convert the DC power to high frequency AC power. The coupling plates consist of a

pair of forward plates and a pair of return plates, they transfer the AC power to the receiver unit. In this design, the load is assumed as AC load, therefore the rectifier is not designed into the receiver unit. The L-match impedance matching circuit is applied at both sides to obtain maximum power transfer. It consists of an inductor and a capacitor, so it also known as LC matching network. This design fulfills the Class- E ZVS condition. Figure 6 shows the flow chart of designing the proposed CPT system.

2.1 Transmitter Unit

In the transmitter unit, the class-E inverter which shown in the Figure 3 is designed by using Simulink in MATLAB. The Class-E inverter is selected to be used in transmitter unit because of its ability to achieve zero-voltage switching (ZVS) which yield 100% efficiency theoretically.

First and foremost, the load resistance, R_L is calculated by Equation (1).

$$R_L = \frac{8\,V_{dc}^2}{(\pi^2+4)P_o} \quad (1)$$

However, in practice the load resistance R_L will not be the same as the calculated value. Therefore, it is crucial to have impedance matching circuit in the CPT system to carry out the impedance transformation to produce a proper load resistance or impedance. The proper load impedance allows the system to match with the source impedance to ensure maximum power transfer in the CPT system, as prescribed by the maximum power transfer theorem assuming there is no internal resistance. The L-match impedance matching circuits shown in Figure 7 are selected to convert the load impedance into required impedance to obtain the desired output power.

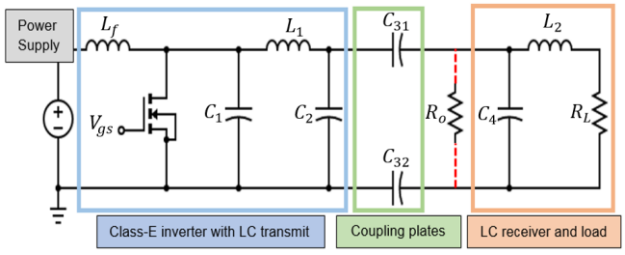

Figure 7 The Class E-LCCL Circuit

2.2 Capacitive Coupling Plates

Capacitor, C_3 is modified and separated into a pair of forward plates and a pair of return plates. Each pair of coupling plates can be represented by a capacitor during simulation. This is because when two metal plates are placed together with a separation either by air or dielectric, it works like a basic capacitor. Consequently, capacitor, C_3 is separated into two capacitors which are capacitor C_{31} and capacitor C_{32} as shown in Figure 7 during simulation. Both capacitors are connected in series and their values are calculated using Equation (2):

$$C_3 = \frac{C_{31}\times C_{32}}{C_{31}+C_{32}} \quad (2)$$

The values of capacitor C_{31} and capacitor C_{32} are equal.

$$C_{31} = C_{32} \quad (3)$$

2.3 Receiver Unit

The receiver unit consists of LC matching circuit and an AC load. Due load is AC, thus there is no rectifier used in this proposed CPT system. The receiver receives and regulates the power to suit the load. The L-match impedance matching circuit matches the load impedance to source impedance to allow maximum power transfer. The receiver unit is shown in Figure 7.

2.4 Assumption and Equations Used in Class-E LCCL Circuit

The design of Class-E LCCL circuit is based on the following assumptions:

I. The MOSFET is ideal which means the on-resistance is zero, off-resistance is infinity, and switching times are zero.
II. The choke inductance is very high that the AC component is much lower than the DC component of the input current.
III. The loaded quality factor, Q of the $L_1 - C_2 - R_L$ series-resonant circuit is high that the current through the resonant circuit is sinusoidal.
IV. All the circuit elements are ideal.
V. Duty cycle is set at 50%.

The proposed CPT system is designed to provide output power $P_O = 10W$ with the operating frequency $f = 1MHz$, DC voltage supply $V_{DC} = 24V$, quality factor $Q = 10$, duty cycle $D = 50\%$ and load resistance $R_L = 50\Omega$. The circuit parameters were calculated based on the equations below:

The series resistance R_S;

$$R_s = \frac{8V_{dc}{}^2}{(\pi^2+4)P_o} = \frac{8(24)^2}{(\pi^2+4)10} = 33.22\Omega \quad (4)$$

The choke inductance L_f ;

$$L_{F(\min)} = 2\left(\frac{\pi^2}{4}+1\right)\frac{R_s}{f} = 2\left(\frac{\pi^2}{4}+1\right)\frac{33.2237}{1\times10^6} = 230.4\mu H \quad (5)$$

And Let $L_f = 500\mu H$ (6)

The shunt capacitance C_1;

$$C_1 = \frac{8}{wR_s\pi(\pi^2+4)} = \frac{8}{(2\pi\times10^6)(33.2237)\pi(\pi^2+4)} = 879.52pF \quad (7)$$

The transmitter matching inductance L_1;

$$L_1 = \frac{Q_L R_s}{w} = \frac{(10)(33.2237)}{(2\pi\times10^6)} = 52.88\mu H \quad (8)$$

The transmitter matching capacitance C_2;

$$C_2 = \frac{Q_L - \frac{\pi(\pi^2-4)}{16} - \sqrt{\frac{R_S\left[\left(Q_L - \frac{\pi(\pi^2-4)}{16}\right)^2 + 1\right]}{R_O} - 1}}{wR_S\left[\left(Q_L - \frac{\pi(\pi^2-4)}{16}\right)^2 + 1\right]} = 474.14\ pF \quad (9)$$

The coupling capacitance C_3;

$$C_3 = \frac{2}{wR_S\left[\left(Q_L - \frac{\pi(\pi^2-4)}{16}\right)^2 + 1\right]} = 120.85pF \quad (10)$$

The receiver matching capacitance C_4 ;

$$C_4 = \frac{L_2}{R_o R_L} = \frac{40.04\ \mu}{(1316)(50)} = 608.55pF \quad (11)$$

The receiver matching inductance L_2 ;

$$L_2 = \frac{\sqrt{R_o R_L - R_L^2}}{2\pi f} = \frac{\sqrt{(1316)(50) - 50^2}}{2\pi 10^6} = 40.04\mu H \quad (12)$$

3.0 RESULTS AND DISCUSSION

This section describes the output performance of the proposed CPT system. The results of the output performance of the system by varying the load, duty cycle, and gap distance between coupling plates are also presented.

3.1 Simulation Results of the Class E LCCL Circuit

The output performances of the proposed CPT system based on calculation and simulation are shown in this section. The design specification calculated and tabulated in Table 1 and 2. The simulation for designed CPT system was carried out using MATLAB shown in Figure 8 and the results are shown in the Table 3. The validity of the proposed CPT system has been verified through calculation as shown in the Table 3.

Table 1 Design Specification

Design specification		
Parameters	**Unit**	**Design value**
f	MHz	1
V_{dc}	V	24
P_o	W	10
R_L	Ω	50
L_F	µH	500
D		0.5
Q_L		10

Table 2 Circuit Parameter

Circuit parameters		
Parameters	**Unit**	**Design value**
R_S	Ω	33.22
C_1	pF	879.52
L_1	µH	52.88
C_2	pF	474.14
C_3	pF	120.85
C_4	pF	608.55
L_2	µH	40.04
$R_o = X_{c3}$	Ω	1316.00

Table 3 Output performance for the proposed CPT system

Output Performance				
Parameters	**Unit**	**Calculation value (theory)**	**Simulation value (MATLAB)**	**% of error**
$V_{RL(peak)}$	V	31.62	31.735	0.36
$I_{RL(peak)}$	A	0.63	0.6345	0.71
$V_{L2(peak)}$	V	159.12	159.70	0.36
$V_{C4(peak)}$	V	162.23	162.80	0.35
$V_{C3(peak)}$	V	162.35	163.40	0.65
$I_{C3(peak)}$	A	0.12	0.1232	2.67
$V_{C2(peak)}$	V	229.52	230.40	0.38
$V_{ds(peak)}$	V	85.39	89.31	4.60
V_{dc}	V	24	24	0
I_{dc}	A	0.42	0.4309	2.60
P_{in}	W	10	10.3416	3.42
P_{out}	W	10	10.0679	0.68
η	%	100	97.35	

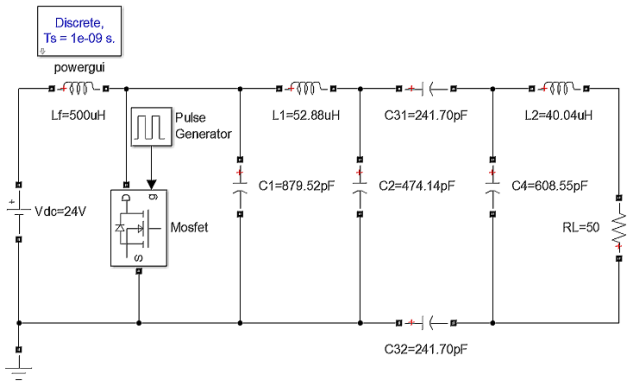

Figure 8 Simulated CPT system in MATLAB

3.1.1 *Zero-voltage Switching*

Zero-voltage Switching (ZVS) basically means when the output voltage is 0V, it turns on or off the power to the load which helps to prolong the life of the controller and of the load being controlled. The theoretical value for the maximum voltage when the MOSFET is turned off is 85.39V. For the simulation results, $V_{ds}(OFF)$ is 89.31V, which is approximately three times larger than the 24 V DC voltage supply, V_{dc} and 4.60% higher than the calculated result. Figure 9 shows the waveforms of the switch voltage V_{ds} and I_{ds}. It clearly shows that there is no overlap between these two waveforms, hence, the ZVS condition is satisfied.

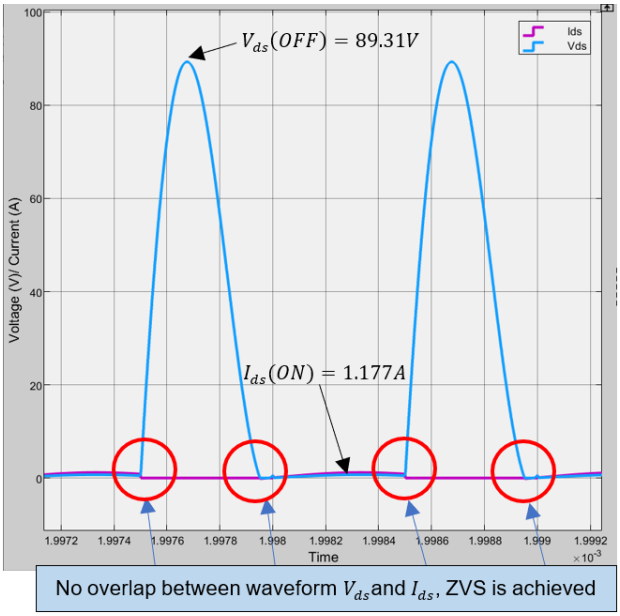

Figure 9 Zero-voltage Switching of CPT system

3.1.2 AC-DC Efficiency of the System

AC-DC efficiency is the ratio of output power in AC, P_{out} to input power in DC, P_{in} as shown in the equation (17) and (18). The efficiency of the system, the output power and input power of the system are calculated based on the equation (13) and (18).

The input power P_{in} is

$$\mathrm{P_{in}(calc.)} = \mathrm{V_{dc}} \times \mathrm{I_{dc}} = 24 \times 0.417 = 10\mathrm{W} \quad (13)$$

$$\mathrm{P_{in}(sim.)} = \mathrm{V_{dc}} \times \mathrm{I_{dc}} = 24 \times 0.4309 = 10.3416\mathrm{W} \quad (14)$$

The output power $\mathrm{P_{out}}$ is

$$\mathrm{P_{out}(calc.)} = \frac{\left(\frac{\mathrm{V_{RL(peak)}}}{\sqrt{2}}\right)^2}{\mathrm{R_L}} = \frac{\left(\frac{31.6228}{\sqrt{2}}\right)^2}{50} = 10\mathrm{W} \quad (15)$$

$$\mathrm{P_{out}(sim.)} = \frac{\left(\frac{\mathrm{V_{RL(peak)}}}{\sqrt{2}}\right)^2}{\mathrm{R_L}} = \frac{\left(\frac{31.735}{\sqrt{2}}\right)^2}{50} = 10.0679\mathrm{W} \quad (16)$$

The efficiency of the system η is

$$\eta(\mathrm{calc.}) = \frac{\mathrm{P_O(ac)}}{\mathrm{P_{in}(dc)}} \times 100\% = \frac{10}{10} \times 100 = 100\ \% \quad (17)$$

$$\eta(\mathrm{sim.}) = \frac{\mathrm{P_O(ac)}}{\mathrm{P_{in}(dc)}} \times 100\% = \frac{10.0679}{10.3416} \times 100 = 97.35\% \quad (18)$$

The proposed CPT is simulated in MATLAB. Figure 10 shows the waveform for input voltage V_{dc} and input current I_{dc} while Figure 11 shows the output voltage V_{RL} and output current I_{RL} for the simulation. All the values contribute to the input power and output power.

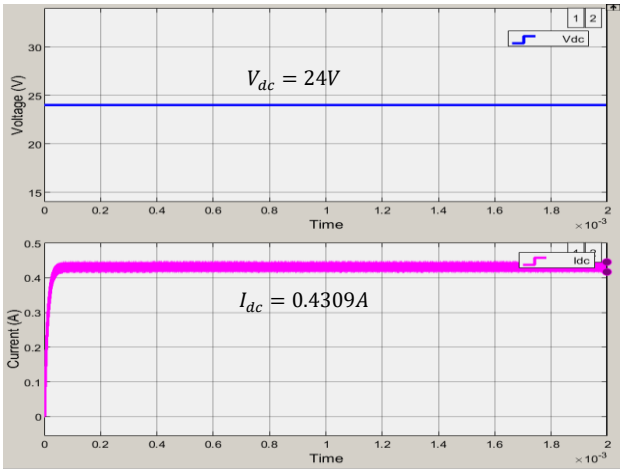

Figure 10 Simulated Input Voltage and Input Current

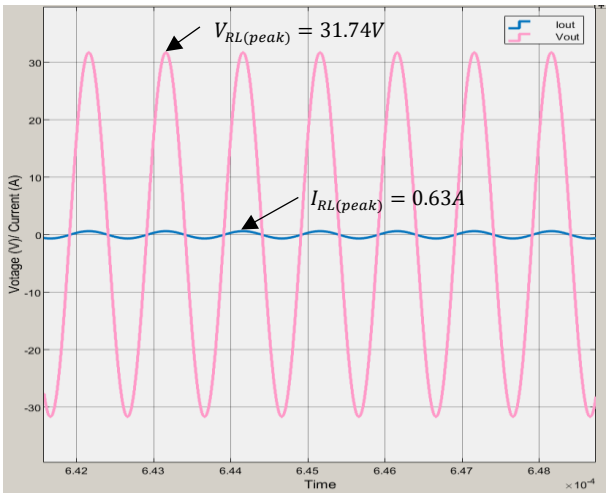

Figure 11 Simulated output voltage and output current

3.2 Analysis of Class-E LCCL Circuit with Load Variation

In the WPT system, the load resistance has a great effect on output voltage and output current. Different range of load resistance is applied based on applications of WPT systems. Therefore, the effects of load variation on the performance of Class-E LCCL power transfer system especially for its output voltage and output current were investigated as shown in the Table 4.

The calculated optimum load, $R_L(opt)$, is 50Ω. To investigate the effects of the load variations, the values of the load resistor in the simulation is set from 5Ω *to* $200\ \Omega$

Table 4 Output performance of the system; (a) at $R_L < R_{opt}$; (b) $R_L = R_{opt}$; (c) at $R_L > R_{opt}$

(a)

Results		$R_L < R_{opt}$				
		Sim.	Sim.	Sim.	Sim.	Sim.
R_L	Ω	5	10	20	30	40
$V_{RL(peak)}$	V	9.225	15.04	22.18	26.555	29.59
$I_{RL(peak)}$	A	1.845	1.504	1.109	0.885	0.7395
$V_{L2(peak)}$	V	463.65	378	278.85	222.6	186.1
$V_{C4(peak)}$	V	463.7	378.25	279.7	224.15	188.4
$V_{C3(peak)}$	V	103	105.5	124.4	141.1	153.9
$I_{C3(peak)}$	A	0.0799	0.0854	0.0973	0.1066	0.1159
$V_{C2(peak)}$	V	373.10	314.05	259.4	239.4	232.55
$V_{ds(peak)}$	V	171.4	124.8	69.24	76.25	83.85
V_{dc}	V	24	24	24	24	24
I_{dc}	A	0.9304	0.7831	0.6183	0.5292	0.4726
P_{in}	W	22.3296	18.7944	14.8392	12.7008	11.3424
P_{out}	W	8.5101	11.3101	12.2988	11.7506	10.9409
η	%	38.11	60.18	82.88	92.52	96.46

(b)

Results		$R_L = R_{opt}$ Sim.
R_L	Ω	50
$V_{RL(peak)}$	V	31.735
$I_{RL(peak)}$	A	0.6345
$V_{L2(peak)}$	V	159.70
$V_{C4(peak)}$	V	162.80
$V_{C3(peak)}$	V	163.40
$I_{C3(peak)}$	A	0.1232
$V_{C2(peak)}$	V	230.40
$V_{ds(peak)}$	V	89.31
V_{dc}	V	24
I_{dc}	A	0.4309
P_{in}	W	10.3416
P_{out}	W	10.0679
η	%	97.35

(c)

Results		$R_L > R_{opt}$				
		Sim.	Sim.	Sim.	Sim.	Sim.
R_L	Ω	80	110	140	170	200
$V_{RL(peak)}$	V	33.275	33.725	33.93	34.045	34.12
$I_{RL(peak)}$	A	0.416	0.3066	0.2424	0.2003	0.1706
$V_{L2(peak)}$	V	104.7	77.15	61	50.35	42.89
$V_{C4(peak)}$	V	109.7	84.05	69.6	60.65	54.70
$V_{C3(peak)}$	V	169.5	171.2	172	172.4	172.60
$I_{C3(peak)}$	A	0.1274	0.1285	0.129	0.1293	0.1295
$V_{C2(peak)}$	V	218.1	213.35	211.25	210.1	209.45
$V_{ds(peak)}$	V	94.21	95.68	96.33	96.68	96.89
V_{dc}	V	24	24	24	24	24
I_{dc}	A	0.2959	0.2213	0.1763	0.1465	0.1254
P_{in}	W	7.1016	5.3112	4.2312	3.516	3.0096
P_{out}	W	6.9212	5.7237	5.2540	3.4096	2.9104
η	%	97.46	97.34	97.19	96.97	96.70

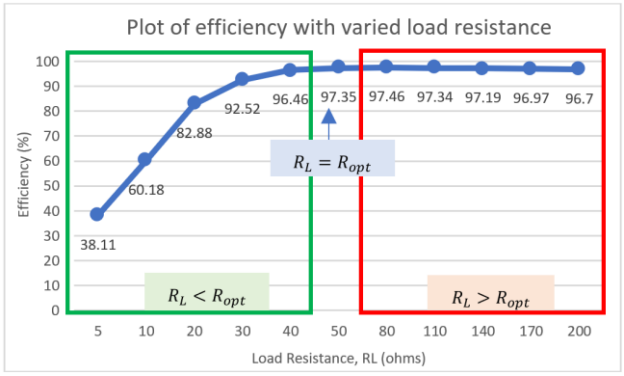

Figure 12 Graph of efficiency vs load resistance

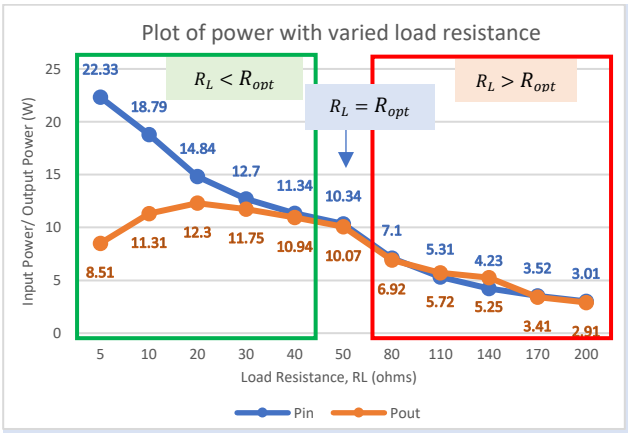

Figure 13 Graph of power vs load resistance

Figure 12 shows the graph of efficiency at each value of load while Figure 13 shows the graph of power for the loads. The efficiency is the ratio of the total output power to the input power. When $R_L < R_{opt}$, the output power of the system is lower than the input power. This implies that the efficiency of the system for $R_L < R_{opt}$ is lower than the efficiencies of the system at $R_L = R_{opt}$. However, the difference between the input power and the output power decreases when R_L approaches R_{opt} which causes the efficiency to increase from 38.11% to 96.46%. The input power decreases due to the decreases in I_{dc}. When $R_L < R_{opt}$, there is a gap for input power P_{in} and output power P_{out}. This is because when the load resistance R_L is smaller than optimum load which is 50Ω for the proposed CPT system, the zero-voltage switching (ZVS) condition is not achieved, the waveforms of the switch voltage, V_{ds} are defective. Thus, the circuit is suffered from extra switching loss. As a result, the output power P_{out} is much lower than the input power P_{in}.

When $R_L = R_{opt}$, the system yields the maximum drain efficiency, which is 97.35% due to no switching loss when the MOSFET turns on and off. The input power and output power at $R_L = R_{opt}$ are high and yield approximately 100% efficiency.

When $R_L > R_{opt}$, there is no major difference between the output power and the input power of the system while the efficiency of system for $R_L > R_{opt}$ is almost constant. In the 2nd block of the Class-E LCCL circuit, the L-match impedance matching circuit was applied and the load, R_L(50Ω) was matched to X_{C3} (1316Ω). The LC impedance matching circuit compensate the power being transferred. Thus, within this limit of load resistanceR_L, which is $50\Omega < R_L < 1316\Omega$, the efficiency of the system remains high and achieve almost 100% efficiency.

3.3 Analysis of Class-E LCCL Circuit with Duty Cycle Variation at 1 MHZ

Duty cycle of the pulse generator is the percentage or ratio of turning on and off a signal. It controls the amount of average DC voltage applied to the MOSFET in the Class-E LCCL power transfer system. Which in turn, affects the performance of Class-E LCCL power transfer system. Therefore, an adjustable duty cycle is useful when the output power needs to be changed without prioritizing the efficiency of the system. In this section, the effect of changing the duty cycle on the output power performance is examined and recorded in Table 5. With similar design specifications outlined in the previous section, the duty cycle, D was controlled within 10% to 90% range.

Table 5 Output performance with variation of duty cycle; (a) Duty cycle 10% to 50%; (b) Duty cycle 60% to 90%

(a)

Results		Duty cycle, D (%)				
		10	20	30	40	50
$V_{RL(peak)}$	V	6.225	11.805	20.98	29.30	31.735
$I_{RL(peak)}$	A	0.1245	0.2362	0.4196	0.586	0.6345
$V_{L2(peak)}$	V	30.655	59.20	105.60	147.50	159.70
$V_{C4(peak)}$	V	31.32	60.45	107.65	150.30	162.80
$V_{C3(peak)}$	V	30.91	59.81	107.90	151	163.40
$I_{C3(peak)}$	A	0.0257	0.0482	0.0830	0.1139	0.1232
$V_{C2(peak)}$	V	45.34	86.70	15.275	212.55	230.40
$V_{ds(peak)}$	V	50.30	61.77	71.68	85.48	89.31
V_{dc}	V	24	24	24	24	24
I_{dc}	A	0.0628	0.1301	0.2517	0.3821	0.4309
P_{in}	W	1.5072	3.1224	6.0408	9.1704	10.3416
P_{out}	W	0.3875	1.3942	4.4016	8.5849	10.0679
η	%	25.71	44.65	72.86	93.62	97.35

(b)

Results		Duty cycle, D (%)			
		60	70	80	90
$V_{RL(peak)}$	V	32	33.79	35.40	33.99
$I_{RL(peak)}$	A	0.64	0.676	0.708	0.68
$V_{L2(peak)}$	V	161.05	170.3	178.55	171.55
$V_{C4(peak)}$	V	164.15	173.45	181.80	174.65
$V_{C3(peak)}$	V	164.80	174.60	184.5	179.30
$I_{C3(peak)}$	A	0.1243	0.13	0.1348	0.1287
$V_{C2(peak)}$	V	232.25	244.70	255.25	244.3
$V_{ds(peak)}$	V	90.05	103.68	186.90	412.5
V_{dc}	V	24	24	24	24
I_{dc}	A	0.4418	0.599	1.2067	4.0404
P_{in}	W	10.6032	14.376	28.9608	96.9696
P_{out}	W	10.24	11.4210	12.5316	11.5566
η	%	96.57	70.45	43.27	11.92

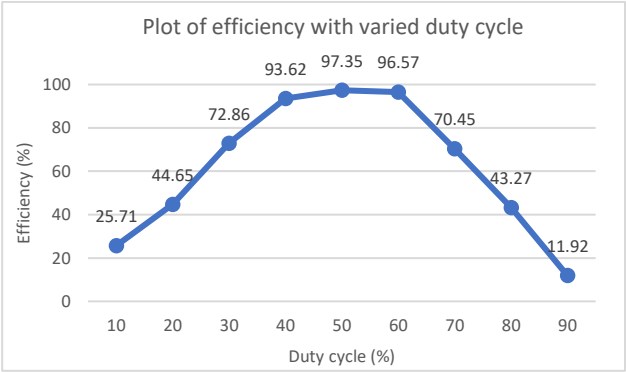

Figure 14 Graph of efficiency vs duty cycle

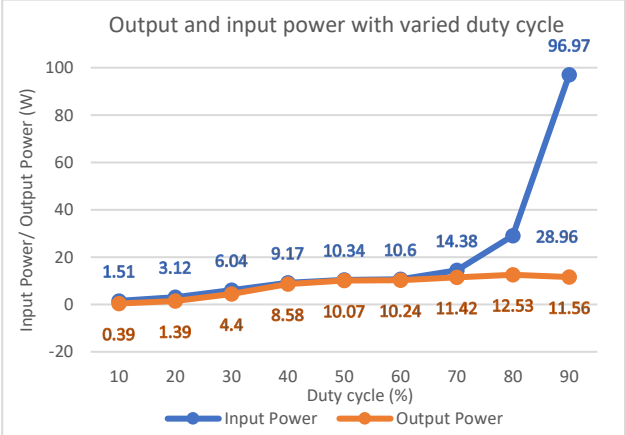

Figure 15 Graph of power vs duty cycle

Figure 14 and Figure 15 show the plot of simulated output performance of Class E LCCL circuit versus duty cycle, D. It can be clearly seen that the maximum output performance is obtained at D=50%. At this point, the efficiency for the simulation is equivalent to 97.35%. For the duty cycle $D < 50\%$ and $D > 50\%$, the input power is much higher than the output power and this causes the efficiency of the system to be less than the efficiency at D=50%.

3.4 Analysis Of Class-E LCCL Circuit with Coupling Variation

The Class E-LCCL system operates at 1 MHz frequency and achieved 100% and 97.35% efficiency via calculation and simulation respectively, was analyzed at 0.07cm coupling gap distance which calculating by using the Equation (3).

$$C_3 = \frac{\varepsilon_o \varepsilon_r A}{d} \tag{19}$$

where,

Permittivity of vacuum,$\varepsilon_o = 8.8542 \times 10^{-12} m^{-3} kg^{-1} s^4 A^2$
Relative permittivity of air, $\varepsilon_r = 1.0006$
Area of the capacitive plate, A=10cm x 10cm=0.01m^2
Capacitance of the coupling plates, C_3=120.85 pF.

Based on Equation (19), the separation distance between the capacitive plates influences the capacitance of both capacitive plates and thus affect the output performance of the Class-E LCCL power transfer system.

The original distance for the proposed CPT system is calculated by utilizing the Equation (19) and the information provided in Table 2. The original distance is calculated as below:

$$d(original) = \frac{\varepsilon_o \varepsilon_r A}{C_3} = \frac{(8.8542 \times 10^{-12})(1.0006)(0.01)}{120.85p} = 0.07cm \quad (20)$$

Hence, the coupling distance is varied from the 0.07cm (original distance) to 10cm to observe the output performance of the system. Table 6 shows the output performance of the proposed CPT system from gap variation of 1cm to 10cm. The output performance for separation distance of 0.07cm can be referred to Table 3.

Table 6 Output performance with coupling variation; (a) 1cm to 4cm; (b)5cm to 7cm; (c) 8cm to 10cm

(a)

Results		Separation distance between capacitive plate (cm)			
		1	2	3	4
C_3	pF	8.8595	4.4298	2.9532	2.2149
C_{31}/C_{32}	pF	17.72	8.86	5.91	4.43
$V_{RL(peak)}$	V	64.40	33.225	17.985	12.075
$I_{RL(peak)}$	A	1.288	0.6645	0.3598	0.2415
$V_{L2(peak)}$	V	319.50	167.2	90.5	60.75
$V_{C4(peak)}$	V	325.75	170.45	92.3	61.95
$V_{C3(peak)}$	V	4450	4651	3772	3378
$I_{C3(peak)}$	A	0.2472	0.1296	0.0702	0.0472
$V_{C2(peak)}$	V	4461	4653.5	3773	3378
$V_{ds(peak)}$	V	220.3	354.4	393.7	399.5
V_{dc}	V	24	24	24	24
I_{dc}	A	3.8878	5.8368	5.1506	4.7916
P_{in}	W	93.3072	140.1264	123.6144	114.9984
P_{out}	W	41.4736	11.0390	3.2355	1.4581
η	%	44.45	7.88	2.62	1.27

(b)

Results		Separation distance between capacitive plate (cm)		
		5	6	7
C_3	pF	1.7719	1.4766	1.2656
C_{31}/C_{32}	pF	3.54	2.95	2.53
$V_{RL(peak)}$	V	9.04	7.22	6.01
$I_{RL(peak)}$	A	0.1808	0.1444	0.1202
$V_{L2(peak)}$	V	45.48	36.32	30.23
$V_{C4(peak)}$	V	46.375	37.035	30.825
$V_{C3(peak)}$	V	3164	3031	2942
$I_{C3(peak)}$	A	0.0353	0.0282	0.0235
$V_{C2(peak)}$	V	3164	3031.5	2942
$V_{ds(peak)}$	V	400.2	399.8	399.3
V_{dc}	V	24	24	24
I_{dc}	A	4.5860	4.4553	4.3655
P_{in}	W	110.064	106.9272	104.772
P_{out}	W	0.8172	0.5213	0.3612
η	%	0.74	0.49	0.34

(c)

Results		Separation distance between capacitive plate (cm)		
		8	9	10
C_3	pF	1.1074	0.9844	0.8860
C_{31}/C_{32}	pF	2.21	1.97	1.77
$V_{RL(peak)}$	V	5.13	4.4985	3.986
$I_{RL(peak)}$	A	0.1027	0.09	0.0797
$V_{L2(peak)}$	V	25.82	22.63	20.055
$V_{C4(peak)}$	V	26.325	23.075	20.45
$V_{C3(peak)}$	V	2876	2828	2789
$I_{C3(peak)}$	A	0.0201	0.0176	0.0156
$V_{C2(peak)}$	V	2876	2828	2789
$V_{ds(peak)}$	V	398.7	398.1	397.6
V_{dc}	V	24	24	24
I_{dc}	A	4.2996	4.2507	4.2108
P_{in}	W	103.1904	102.0168	101.0592
P_{out}	W	0.2634	0.2024	0.1588
η	%	0.26	0.20	0.16

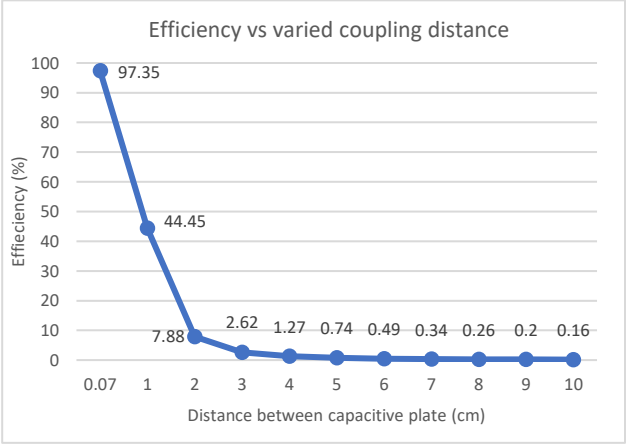

Figure 16 Graph of efficiency vs coupling distance variation

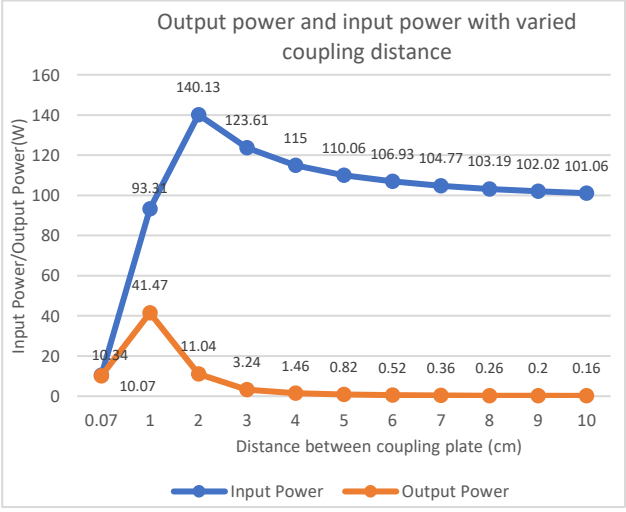

Figure 17 Graph of power vs coupling distance variation

Figure 16 shows the system efficiency while Figure 17 shows the related input and output power when the coupling plates distance were varied from 0.07 cm to 10 cm. The results show that increasing the distance between the coupling plates reduces the emission field energy while decreasing the value of capacitance of the coupling plates, C_3. Based on Equation (19), the capacitance of the coupling plates is inversely proportional to the separation distance between the plates, d. When the distance increase between plates, d, the capacitance of coupling plates, C_3, decreases which reduces the output current, and in turn reduces the output voltage. t can be observed there is extremely reduction in efficiency and slightly decrement in the power when the plated distance is varied from 0.07 cm to 3 cm.

4.0 CONCLUSION

A CPT system with a Class-E LCCL inverter and L-match impedance matching network was successfully developed and presented. The system operates at 1 MHz frequency, gap distance of 0.07cm and 24 V power supply. The system achieved the ZVS condition which yields a high efficiency of 100% theoretically and 97.35% in the simulation. In this study, the efficiency and output power of the system was shown to be affected by load variation, duty cycle variation, and gap distance variation. For the load variation, the maximum power transfer was achieved at optimum load ($R_L = 50\Omega$) and yields a high efficiency of 97.35%. For loads less than the optimum load ($R_L < 50\Omega$), the efficiency of the system is lower than the efficiency of the optimum load. However, for loads higher than the optimum load ($R_L > 50\Omega$), the efficiency of the system is high which is above 96% due to the compensation of the L-match impedance matching circuit at receiver unit. In the duty cycle variation, it was shown that the maximum power transfer can be only achieved at 50% duty cycle. In the last experiment with the gap distance variation, it was found that when the distance between the coupling plates increases, the efficiency of the system decreases. This requires extra effort in designing a proper circuit to handle this issue. We include this as future work. In conclusion, in order to allow maximum power transfer from source to load, the designed CPT system must operate at optimum load, 50% of duty cycle and as smaller as coupling gap distance. Last but not least, the findings in this paper have shown the greater possibilities of the WPT technology. in the conclusion.

Acknowledgement

This research was supported by the Universiti Teknikal Malaysia Melaka (UTeM) and Ministry of Science, Technology and Innovation for sponsoring this work under the Fundamental Research Grant Scheme [FRGS/1/2021/FKEKK/F00473]

References

[1] C. H. Lee, G. Jung, K. Al Hosani, B. Song, D. K. Seo, and D. Cho. 2020. Wireless Power Transfer System for an Autonomous Electric Vehicle. *2020 IEEE Wireless Power Transfer Conference, WPTC 2020*. 467-470. Doi: 10.1109/WPTC48563.2020.9295631.

[2] Z. Zhang, H. Pang, A. Georgiadis, and C. Cecati. 2019. Wireless Power Transfer - An Overview. *IEEE Trans. Ind. Electron.* 66(2): 1044-1058. Doi: 10.1109/TIE.2018.2835378.

[3] J. Lopez-Lopez, C. Salto, P. Zumel, C. Fernandez, A. Rodriguez-Lorente, and E. Olias. 2018. High Efficiency Capacitive Power Transfer Converter. *Conf. Proc. - IEEE Appl. Power Electron. Conf. Expo. - APEC*. 2018: 3149-3153. Doi: 10.1109/APEC.2018.8341551.

[4] F. C. Domingos, S. Vital, D. C. De Freitas, and P. Mousavi. 2018. Capacitive Power Transfer based on Compensation Circuit for Class E Resonant Full-Wave Rectifier. *2018 IEEE Wirel. Power Transf. Conf*. 1-4.

[5] Y. Zhao, B. Mahoney, and J. R. Smith. 2016. Analysis of a Near Field Communication Wireless Power System. *2016 IEEE Wirel. Power Transf. Conf. WPTC 2016*. 2-5. Doi: 10.1109/WPT.2016.7498827.

[6] I. Ramos, K. Afridi, J. A. Estrada, and Z. Popović. 2016. Near-field Capacitive Wireless Power Transfer Array with External Field Cancellation. *2016 IEEE Wirel. Power Transf. Conf. WPTC 2016*. 4-7. Doi: 10.1109/WPT.2016.7498829.

[7] C. Liu, Y. X. Guo, H. Sun, and S. Xiao. 2014. Design and Safety Considerations of an implantable Rectenna for Far-field Wireless Power Transfer. *IEEE Trans. Antennas Propag.* 62(11): 5798-5806. Doi: 10.1109/TAP.2014.2352363.

[8] P. S. Yedavalli, T. Riihonen, X. Wang, and J. M. Rabaey. 2017 Far-Field RF Wireless Power Transfer with Blind Adaptive Beamforming for Internet of Things Devices. *IEEE Access*. 5: 1743-1752. Doi: 10.1109/ACCESS.2017.2666299.

[9] Y. Yusop *et al.* 2016. A Study of Capacitive Power Transfer Using Class-E Resonant Inverter. *Asian J. Sci. Res.* 9(5): 258-265. Doi: 10.3923/ajsr.2016.258.265.

[10] V. T. Nguyen, S. D. Yu, S. W. Yim, and K. Park. 2017. Optimizing Compensation Topologies for Inductive Power Transfer at Different Mutual Inductances. *2017 IEEE PELS Work. Emerg. Technol. Wirel. Power Transf. WoW 2017*. 1: 153-156. Doi: 10.1109/WoW.2017.7959384.

[11] Third International Conference on Properties and Applications of Dielectric Materials. 1992. *IEEE Transactions on Electrical Insulation*. 27(3). Doi: 10.1109/14.142698.

[12] A. Aldaoud *et al.* 2018, Near-Field Wireless Power Transfer to Stent-Based Biomedical Implants. *IEEE Journal of Electromagnetics, RF and Microwaves in Medicine and Biology*. 2(3): 193-200. Doi: 10.1109/JERM.2018.2833386.

[13] Z. Mustapa, S. Saat, and Y. Yusof. 2019. A New Design of Capacitive Power Transfer based on Hybrid Approach for Biomedical Implantable Device. 9(4): 2336-2345. Doi: 10.11591/ijece.v9i4.pp2336-2345.

[14] B. Jalali and A. Mahjoubfar. 2015. Tailoring Wideband Signals with a Photonic Hardware Accelerator. *Proceedings of the IEEE*. 103(7): 1071-1086. Doi: 10.1109/JPROC.2015.2418538.

[15] F. Lu, H. Zhang, H. Hofmann and C. Mi. 2016. A CLLC-Compensated High Power and Large Air-gap Capacitive Power Transfer System for Electric Vehicle Charging Applications. 2016 IEEE Applied Power Electronics Conference and Exposition (APEC). 1721-1725. Doi: 10.1109/APEC.2016.7468099.

[16] B. Luo, T. Long, L. Guo, R. Dai, R. Mai, and Z. He. 2020. "and Design of Inductive and Capacitive Hybrid Wireless Power Transfer System for Railway Application. *IEEE Trans. Ind. Appl.* 56(3): 3034-3042. Doi: 10.1109/TIA.2020.2979110.

[17] B. Regensburger, A. Kumar, S. Sinha, and K. Afridi. 2018. High-Performance 13.56-MHz Large Air-gap Capacitive Wireless Power Transfer System for Electric Vehicle Charging. *2018 IEEE 19th Work Control Model. Power Electron. COMPEL 2018*. 1-4. Doi: 10.1109/COMPEL.2018.8460153.

[18] H. Zhang, C. Zhu, S. Zheng, Y. Mei, and F. Lu. 2019. High Power Capacitive Power Transfer for Electric Aircraft Charging Application. *Proc. IEEE Natl. Aerosp. Electron. Conf. NAECON*. 2019-July(c): 36-40. Doi: 10.1109/NAECON46414.2019.9057957.

[19] T. M. Mostafa, A. Muharam and R. Hattori. 2017. Wireless Battery Charging System for Drones via Capacitive Power Transfer. *2017 IEEE PELS Workshop on Emerging Technologies: Wireless Power Transfer (WoW)*. 1-6. Doi: 10.1109/WoW.2017.7959357.

[20] Y. Yusop, S. Saat, Z. Ghani, H. Husin, and S. K. Nguang. 2019. Cascaded Boost-Class-E for Rotary Capacitive Power Transfer System. 3742-3748. Doi: 10.1049/joe.2018.8016.